Zeitschrift: IABSE reports = Rapports AIPC = IVBH Berichte

Band: 67 (1993)

Artikel: Analytical modelling for fatigue assessment of the Clifton suspension bridge

Autor: Cullimore, M.S.G. / Mason, Peter J. / Smith, William J.

DOI: https://doi.org/10.5169/seals-51377

Analytical Modelling for Fatigue Assessment of the Clifton Suspension Bridge

Modèle analytique d'évaluation de la fatigue du pont suspendu de Clifton

Analytisches Modell zum Ermüdungszustand der Clifton-Hängebrücke

M.S.G. CULLIMORE
Visiting Research Fellow
University of Bristol
Bristol, UK

M. Stuart Cullimore, born 1920, graduated in civil engineering from Bristol University in 1940. Reader in Structural Engineering until 1985. Reserach latterly on fatigue of structural joints and bridge decks. Now Visiting Fellow at University of Bristol.

Peter J. MASON
Director
Howard Humphreys & Partners
Dorking, UK

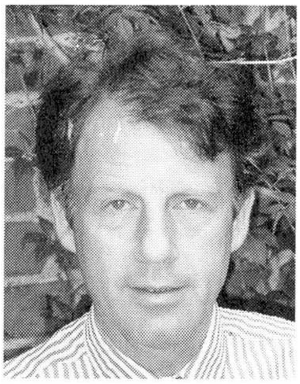

Peter Mason, born 1945, joined the Bridge Department of Howard Humphreys & Partners, consulting engineers, in 1967 on graduating from Imperial College, London. He is now a director of the company and is responsible for all the firm's structural engineering work.

J. William SMITH
Senior Lecturer
University of Bristol
Bristol, UK

William Smith, born 1941, graduated in Civil Engineering at the University of Edinburgh, Scotland. Obtained his PhD (vibration of bridges) at the University of Bristol where he now studies dynamic loading and fatigue of bridges.

SUMMARY

The Clifton Suspension bridge is an iron eye-bar chain suspension bridge of 214 m span. Despite its age (128 years) it is a vital link in the traffic system of Bristol, carrying nearly 4 million vehicles per year. An extensive structural assessment of the bridge has been carried out. This has required global analytical modelling, load testing, strain monitoring under traffic, and fatigue appraisal of the major components.

RÉSUMÉ

D'une portée de 214 m, le pont suspendu de Clifton est supporté par des chaînes formées de barres à oeil. Malgré son âge de 128 ans et avec près de 4 millions de véhicules par année, il constitue un élément de liaison essentiel pour le trafic routier de Bristol. Au cours de l'évaluation de la sécurité à la ruine à l'aide d'un modèle analytique appliqué à la structure complète, il a été procédé à des essais de charge et à des mesures de déformation sous charge mobile, ainsi qu'à la vérification de la fatigue de tous les éléments porteurs principaux.

ZUSAMMENFASSUNG

Die Clifton-Hängebrücke mit 214 m Spannweite wird von Ketten aus eisernen Augenstäben getragen. Trotz ihres Alters von 128 Jahren stellt sie mit fast 4 Mio. Fahrzeugen pro Jahr eine Hauptverbindung im Verkehrsnetz von Bristol dar. Bei der notwendigen Tragsicherheitsüberprüfung anhand eines analytischen Modells des gesamten Tragwerks wurden Probebelastungen, Dehnugsmessungen unter Verkehr und Ermüdungsnachweise aller Hauptkomponenten durchgeführt.

1. INTRODUCTION

The Clifton Suspension Bridge was designed originally by the eminent Victorian engineer Isambard Kingdom Brunel. The bridge was completed in 1864, after his death, with a number of important modifications to his design [1]. The spectacular setting of the bridge spanning the Avon Gorge makes it an important tourist attraction and focus of civic pride (Fig 1). But it is also an important link in the traffic system of Bristol carrying nearly 4 million vehicles per year, although there is a gross weight limit of 40 kN.

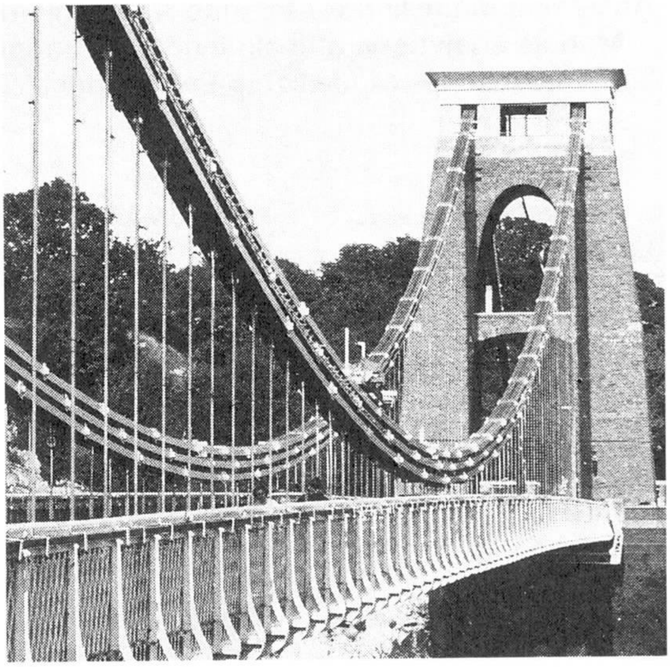

Fig 1 Clifton Suspension Bridge

Structurally the bridge is a wrought iron eye-bar suspension chain with a suspended structure carrying an asphalt surfaced timber deck (Fig 2). There are three chains on each side of the roadway, arranged one above the other as shown in Fig 1. They are made up of 175mm x 25mm wrought iron bars with special eye joints forged to each end. Each link is made up of ten or eleven bars arranged side by side, interleaved with the bars of the next link, and connected with a pin through the eye joint. Successive suspender rods, at intervals of 2.44m (8 feet) are attached to each of the three chains in turn, (see Fig 1), so that the eye-bars are approximately 24 feet in length depending on the local slope of the chain. The wrought iron suspended structure (Fig 2) consists of longitudinal riveted plate girders, under each set of chains, lattice cross-girders and longitudinal lattice parapet girders. The roadway deck is timber with mastic asphalt surfacing.

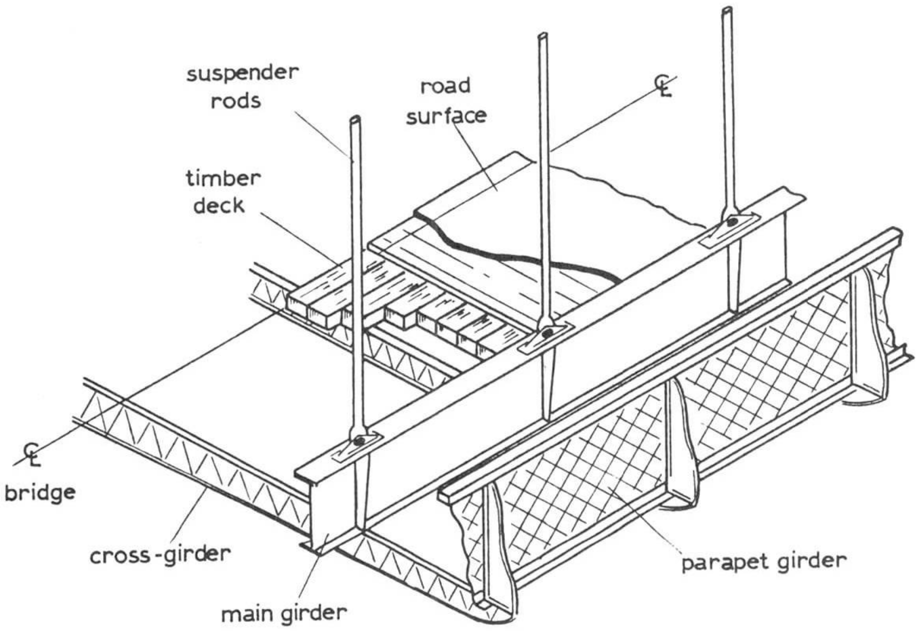

Fig 2 The suspended structure

A number of studies of the structural capacity of the bridge have been undertaken this century, some of them resulting in remedial or strengthening works [1,2]. The collapse of the Point Pleasant Bridge over the Ohio river in 1967, resulting from corrosion-fatigue in an eye bar, prompted an extensive fatigue appraisal of the Clifton Bridge [3]. It was concluded that there was an adequate margin of safety against fatigue failure at that time. However, traffic loading was steadily increasing and there was concern over progressive deterioration of the riveted joints of the parapet girder and other signs of wear or damage. It was decided that a global analysis of the structure should be carried out, using modern analytical methods, so that the effects of a range of load cases could be studied.

2. FINITE ELEMENT MODEL

2.1 Modelling assumptions and analytical procedure

Suspension bridge behaviour under load is geometrically non-linear. This is because the cable or chain adapts its shape when a concentrated load is applied at a particular point on the structure. In most suspension bridges, as at Clifton, the longitudinal girder provides some stiffening and effectively distributes these deformations over part of the structure. For this reason it was decided to use a finite element program which had geometrically non-linear solution capabilities.

The finite element model was designed to represent the effects of vertical loading on the structure. For this purpose a two-dimensional model was considered to be adequate. Dead load and traffic load in both lanes is symmetrical about the longitudinal axis of the bridge and therefore only one half of the bridge needed to be modelled, i.e. one set of three chains supporting the main girder and parapet girder. Eccentric traffic loads, in the form of single vehicles or traffic in one lane only, were dealt with by means of a separate torsional analysis.

A schematic diagram of the node and element geometry is shown in Fig 3a. From the left anchorage to the tower the three chains were represented by a single chain of beam elements. The final link was connected by a pin joint to the saddle elements. The saddle nodes were all effectively constrained to move horizontally as a single unit, simulating the roller bearing that exists at the top of each tower. The three chains of the main span were represented by beam elements of the same length as each eye bar link. Thus the correct sequence of connection to the suspender rods could be modelled as shown. Each link of ten, eleven or twelve bars, was modelled by a single element of equivalent area. It has been observed that the chain links behave as if they are rigidly connected to each other over the main part of the span. The pins work freely only at the tower saddles. The main girder was modelled by beam elements pin connected to the vertical rods as shown. There is no vertical or horizontal restraint to movement of the main girders of the bridge. However, in order to avoid computational instability, a soft horizontal spring restraint was connected to the middle node of the deck.

The behaviour of the cross girders and parapet girder were modelled by suspending longitudinal beam elements from the main girder elements by means of vertical linkages. The stiffness of the linkage elements was determined from the stiffness of the cross girder in shear between points of connection of the main and parapet girders as shown in Fig 3b. In order to avoid the problem of horizontal instability it was sufficient to introduce horizontal coupling between main and parapet girders at mid-span.

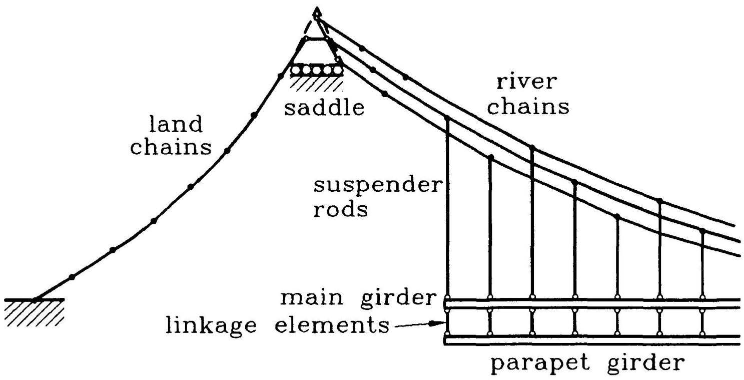

(a) Schematic diagram of node and element geometry

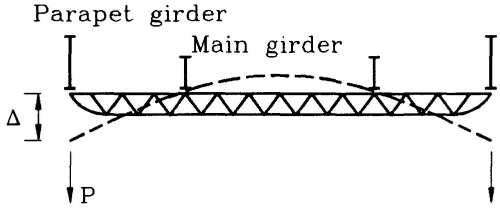

Stiffness of linkage element, k = P/Δ

(b) Modelling of cross-girder stiffness

Fig 3 Finite Element Model

2.2 Analysis of eccentric loading

It was mentioned earlier that eccentric loads, such as single vehicles or traffic in one lane only, could be dealt with by introducing a torsional component. This is illustrated in Fig 4 where it can be seen that the loading can be resolved into symmetric and torsional components at the line of the chains. If the cross girder is rigid, then because of its rotation about the centre line, it forces the parapet girder to deflect more than the main girder in the torsional case. Hence the effective stiffness of the parapet girder, if it is transposed to the same plane as the main girder and the chains, becomes:

$$I_{effPa} = I_p(B/b)^2 \tag{1}$$

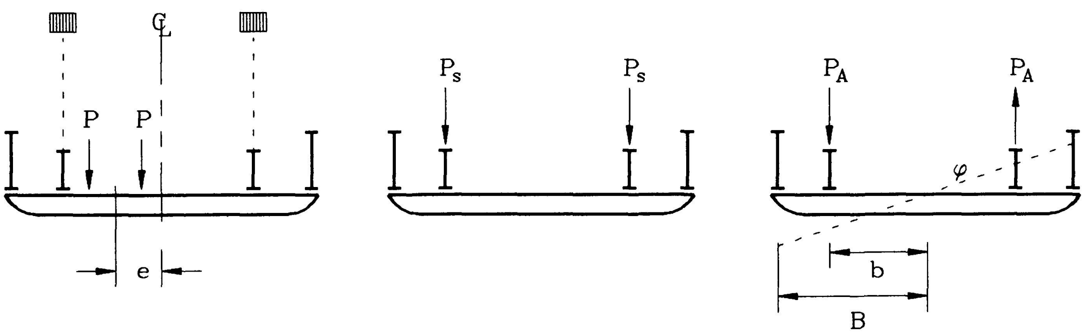

Symmetric component $P_s = P$

Torsional component $P_A = P.e/b$

Fig 4 Analysis of eccentric loading

In this way it would be possible to analyse the problem as two separate load cases and add the results, provided that it could be assumed that deflection of the chains was linear with changes in live load applied at a point. In practice it was possible to combine the symmetric and torsional components into a single eccentric load case. This was done by evaluating the effective stiffness of the parapet girder when transposed to the line of the chains with both symmetric and torsional component loads present. The formula is as follows:

$$I_{effp} = I_p \left[\frac{B^2}{B^2 + fb^2} \right] (1 + f) \; ; \quad \text{where} \quad f = P_a/P_s \qquad (2)$$

Further refinements were included which took account of cross girder flexibility in the torsional case, but are outside the scope of this paper.

2.3 Load tests and comparison with analytical model

In order to confirm the analytical model, loading tests were carried out on the bridge at night. The weight limit on the bridge is 40 kN. This represents vehicles such as ambulances, loaded vans and pick-up trucks. Two loading cases were identified as follows:

(a) Dual vehicle symmetric loading

The maximum concentrated load occurs when two 40 kN vehicles, travelling in opposite directions, pass each other on the span. Assuming a load distribution of 15 kN at front axles and 25 kN at rear axles the load case is as shown in Fig 5. Although the front axles are in opposite lanes of the carriageway, and would produce an anti-symmetric torsional component of loading, it was assumed that this would be a small localised effect and that the load could be treated as symmetric as shown.

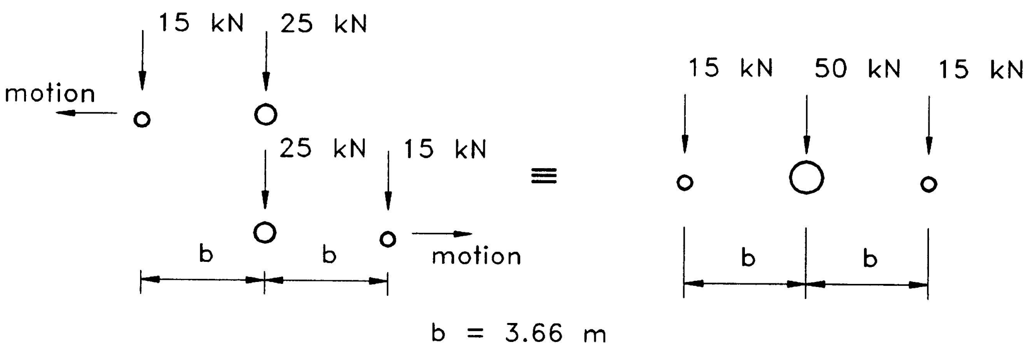

Fig 5 Dual vehicle load case (symmetric)

(b) Single vehicle eccentric loading

The bridge is torsionally flexible and therefore it was considered important to study the effects of a single 40 kN vehicle travelling in one lane of the carriageway, thereby applying an eccentric loading to the structure. The eccentricity of the vehicle in the analysis was taken as 1.0 m from the centre line of the carriageway.

For the loading tests on the bridge, two pick-up trucks were hired and loaded with boxes of nails to provide the appropriate distribution. Strain gauges were fixed to the top and bottom flanges of one parapet girder and both main girders at 1/4 span. The signals were logged by a computer data acquisition system while the vehicles were crossing the span in the loading configurations described above.

The results of a typical analysis are shown in Fig 6 and the results of a single vehicle load test run are shown in Fig 7. Similarity in the shapes of the curves is evident. The test run results are effectively influence lines for strain at 1/4 span when the vehicle passes over the span. The analysis represents the distribution of deflection and bending moments when the vehicle is stationary at the 1/4 point. But since the wheel base of the vehicle is very short compared with the span, and there is evidence of linearity under live loads, it may be considered that the analysis results approximate to influence lines. It may also be noted that the bending in the main girder is sharper than that of the parapet girder directly under the load. This is because flexibility of the cross girder results in transfer of bending from the main to parapet girder to be distributed longitudinally to some extent. A further point to note about the results is that the parapet girder bending moment is of the same order as that of the main girder. It is not known if this structural action of the parapet girder was taken into account in the original design.

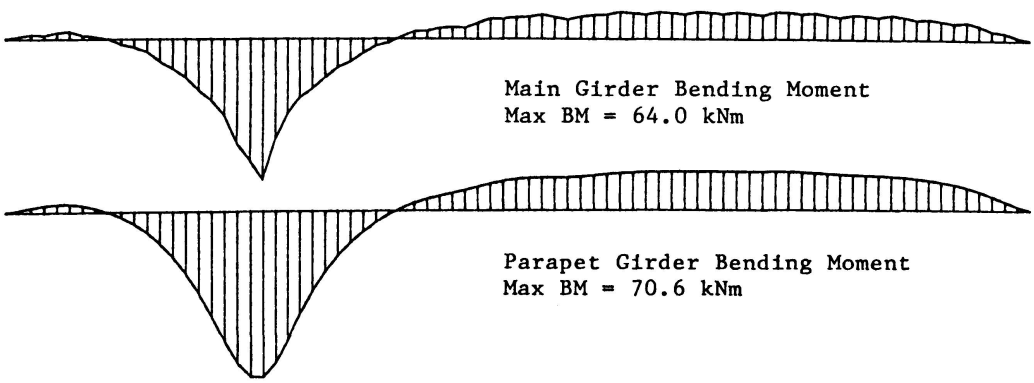

Fig 6 Finite element analysis of eccentric 40 kN load at 1/4 span

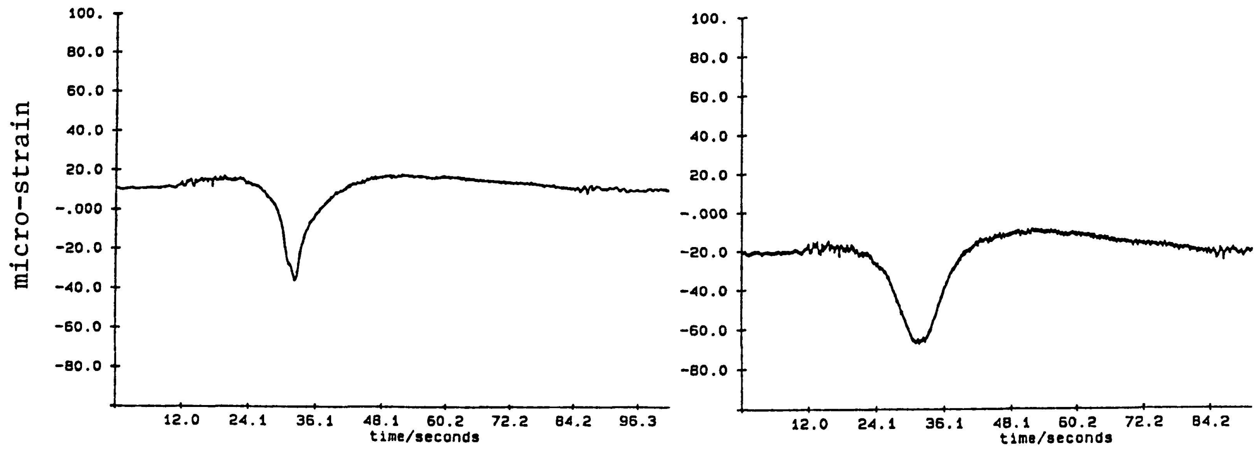

(a) Main Girder (bottom) (b) Parapet Girder (bottom)

Fig 7 Strains at 1/4 span under action of 40 kN vehicle eccentric load

In order to obtain quantitative comparison between the experimental results and the analysis it was necessary to convert the observed strains at top and bottom of the girders to equivalent bending moments. This was done using the measured sectional properties of the girders and a value of E for wrought iron of 192 GN/m^2. The results are compared in Table 1 below.

Table 1 Bending Moments at 1/4 span in kNm (analysis in parentheses)

LOAD	POSITION	MAIN GIRDER		PARAPET GIRDER		TOTAL MOMENT	
8 ton	1/2 span	18.2	(19.7)	13.1	(24.6)	38.4	(44.3)
symm.	3/8 "	3.3	(4.0)	5.3	(1.8)	11.6	(5.8)
	1/4 "	-89.1	(-111.7)	-64.1	(-86.3)	-170.6	(-198.0)
	1/8 "	-2.1	(-8.5)	-7.0	(-10.6)	-18.8	(-19.1)
4 ton ecc.	1/4 "	-56.4	(-64.0)	-43.7	(-70.6)	-111.2	(-134.6)

In Table 1 the experimental moments were evaluated from the strain gauge data so as to provide a comparison with the analysis. The analytical results are generally greater than the experimental results. This is probably a result of the influence of the deck which acts like an additional flange to the main girder. This was difficult to include in the analytical model although some allowance was made by modifying the girder section properties to simulate the shift of the neutral axis.

The 'Total Moment' in Table 1 is the sum of the girder moments in the case of the analysis. However, the longitudinal forces introduced by the presence of the deck could be evaluated from the strain gauge data together with the girder moments. Hence, the 'Total Moment' of the experimental results is always greater than the direct sum of the girder moments.

3. CONTINUOUS MONITORING OF GIRDER STRAINS UNDER NORMAL TRAFFIC

3.1 Installation and use of "Stress Analyser"

The same strain gauge locations, as used in the vehicle loading tests, were monitored continuously under normal traffic for several one week periods. The equipment for doing this, called a "Stress Analyser" [4], was capable of amplifying the signal from the gauges, detecting peaks and troughs of the fluctuating signal, and performing a "rainflow" count in real time. "Rainflow" counting is an accepted method for interpreting a varying amplitude signal in terms of an equivalent number of simple cycles of different amplitudes. The fatigue damaging potential of the signal may then be assessed by summing the fatigue damage contributions of all the simple cycles.

The data are provided in the form of numbers of cycles of different strain ranges. The mean strain was not recorded because, although it has an effect it is generally accepted that, for materials such as wrought iron with many defects, strain range is the dominant factor affecting fatigue life.

3.2 Prediction of strain range cycle count and comparison with observations

The results of the global analysis were used to make a prediction of the strain range cycle count under normal traffic. This was achieved by looking at the output from the analysis of the bridge under a 40 kN eccentric load as shown in Fig 6. It has already been said that this figure approximates to an influence line and therefore the range of bending moment at the 1/4 span when a 40 kN vehicle crosses the bridge may be deduced from the maximum and minimum of this figure. It was further assumed that the bending moments at this point were linear with load within the range of live loading. Hence, it was possible to evaluate strain ranges occurring under the passage of a range of vehicle weights as they cross the bridge.

A classification count was carried out on the bridge, grouping weekday traffic into seven weight classes. Cars were relatively easy to classify according to weight, but estimates had to be made for larger vehicles such as pick-up trucks, vans and ambulances. A count was also made of the number of times vehicles travelling in opposite directions were applying load to a particular cross girder simultaneously. The count is set out in Table 2 below.

Table 2 Number of loadings of a cross girder by vehicles of different weight

Vehicle weight	8	10	14	20	25	30	40 (kN)
Left lane	264	633	252	26	22	11	2
Right lane	343	819	243	41	22	11	3
Both	21	184	56	10	1		

The weights were converted into strains at the top of the main girder and a table of the number of loading cycles within strain range bands was compiled. Data on the number of vehicle crossings was available from the toll records and amounted to 72,000 vehicles per week during the period of the study. The number of cycles for the short count (four hours in total) was then factored up to give the number of cycles that would occur at the same rate during one week of normal traffic. The predicted cycle count was compared with the data obtained using the "Stress Analyser" and is shown in Table 3.

Table 3 Strain range cycle count: Predicted v. Stress Analyser

Strain Range ($\times 10^{-6}$)	Number of Loading Cycles: Predicted, Short count	Predicted, Seven days	Stress Analyser (avg of 3 seven day periods)
0 - 10	343	8,332	124,022
10 - 20	1,326	32,210	20,713
20 - 30	695	16,882	12,403
30 - 40	469	11,393	6,989
40 - 50	82	1,992	3,328
50 - 60	25	607	1,356
60 - 70	21	510	519
70 - 80	1	24	174
80 - 90	2	48	59
90 - 100			18
100 - 110			7
110 - 120			3
120 - 130			1

Considering the difficulties of assessing the loads from the visual classification count the correlation is remarkably good. The large number of cycles occurring in the smallest strain range may be the result of small vibrations and electronic noise. A further comparison can be made by evaluating the fatigue damage done by each loading cycle. This can be achieved by assuming a power law for fatigue life with an index of 3, together with Miner's law of cumulative damage. It is then possible to calculate the equivalent strain range per vehicle, if applied repetitively, that would yield the same fatigue damage as the actual variable loads. This quantity (ESRV) is given by

$$\mathrm{ESRV} = (n_i S_i^{m}/72{,}000)^{1/m} \qquad (3)$$

where n_i is the number of cycles of strain range S_i and m is the index of the power law. $m=3$ is a reliable mean value for fatigue of wrought iron.

Using the data in Table 3 the following comparison may be made:

ESRV predicted = 26.4×10^{-6}
ESRV experiment = 26.8×10^{-6}

This result confirms that the method of prediction provides a very accurate measure of fatigue damage.

4. FATIGUE ASSESSMENT OF MAJOR COMPONENTS

4.1 Saddle link

Rotation of the chain links attached to the saddle bearings at the tops of the towers were found to produce significant variations in principal stress while vehicles crossed the bridge. In an earlier study this was found to be the most significant fatigue loading on the bridge [3]. The results of the load tests carried out on the bridge at that time were found to compare favourably with the global analysis. Hence the conclusion of the earlier assessment, that there was sufficient factor of safety against fatigue or fracture, was confirmed.

4.2 Main girders

The strains observed in the main girder under normal traffic (Table 3) were converted to stress cycles. These were compared with S-N curves for riveted girders [5,6]. Assuming traffic totalling 4 million vehicles per year the fatigue life of the main girder was calculated to be 468 years.

4.3 Parapet girders

For fatigue loading the critical location is the spliced joint in the top flange of the parapet girder. Strains were obtained using the same procedure as for the main girders and were converted to stress ranges. The joints have been progressively deteriorating in recent years and a new friction grip bolted assembly has been designed as a replacement. Using the current UK code for fatigue assessment, the life of the joint was estimated to be 197 years.

REFERENCES

1. MITCHELL-BAKER D and CULLIMORE M S G., Operation and maintenance of the Clifton Suspension Bridge. Proc Inst Civil Engrs, Part 1, n 84, 291-308, April 1988.

2. FLINT A R and PUGSLEY A G., Some experiments on Clifton Suspension Bridge. Correlation between calculated and observed stresses and displacements in structures. Inst Civil Engrs, Preliminary vol, 124-134, London 1955.

3. CULLIMORE M S G and MASON P J., Fatigue and fracture investigation carried out on the Clifton Suspension Bridge. Proc Inst Civil Engrs, Part 1, n 84, 309-329, April 1988.

4. WASTLING M A and SMITH J W., An instrument for detecting arbitrary peaks and troughs of a fluctuating stress signal. Strain, Brit Soc Strain Measurement, 127-131, August 1987.

5. BRUHWILER E, SMITH I F C and HIRT M A., Fatigue and fracture of riveted bridge members. J.Struct.Engng., ASCE, v116, n1, 198-214, 1990.

6. FISHER J W, YEN B T and WANG D., Fatigue strength of riveted bridge members. J.Struct.Engng., ASCE, v116, n11, 2968-2981, 1990.